

PRODUCTION AND STUDY OF POLYETHER AUXETIC FOAM

SUMMARY

The article describes the experiment consisting in production and study of auxetic open-cell polyether foam. In the introduction I briefly explain what auxetic materials are and list their main properties together with possible application areas. Next, detailed information about the background of the experiment is given: important material characteristics and extensive description of the procedure. Further, discussion of the results is presented, basing on microscopic imagery of the obtained auxetic foam. The article describes also tensile tests performed on the produced material and cites quantitative results in the form of text and graphs illustrating the Poisson ratio dependence on deformation, as well as stress-strain relations (true and engineering values). In the final part of the article conclusions are enclosed.

Keywords: negative Poisson's ratio, auxetic materials, open cell polyether foam, auxetic polymer foam, microscopic imagery, tensile test

EKSPERYMENTALNE WYTWORZENIE I BADANIE WŁAŚCIWOŚCI POLIETEROWEJ PIANKI AUKSETYCZNEJ

Artykuł opisuje eksperyment polegający na laboratoryjnym wytworzeniu i badaniu właściwości auksetycznej otwartokomórkowej pianki polieterowej. We wstępie krótko opisane jest, czym są materiały auksetyczne, podane są ich najważniejsze własności oraz możliwe obszary zastosowań. Następnie przedstawione są szczegółowo informacje o samym eksperymencie: scharakteryzowano użyty materiał i przedstawiono sposób wytworzenia pianki. W kolejnej części artykułu znajdują się mikroskopowe obrazy struktury pianki wraz z komentarzem dotyczącym mechanizmów deformacji. Opisany jest także test na rozciąganie otrzymanej pianki auksetycznej; wyniki opatrzone są komentarzem oraz wykresami. Wykresy ilustrują zależności współczynnika Poissona od odkształcenia oraz relację naprężeń i odkształceń (inżynierskich oraz rzeczywistych). W ostatniej części zamieszczono uwagi podsumowujące.

Słowa kluczowe: ujemny współczynnik Poissona, materiały auksetyczne, otwartokomórkowa pianka polieterowa, auksetyczna pianka polimerowa, obrazy mikroskopowe, test na rozciąganie

1. INTRODUCTION

Poisson's ratio – definition, range

Poisson's ratio ν is defined as minus the ratio of transverse strain to longitudinal strain for a material undergoing tension in the longitudinal direction. Of course, the above definition of Poisson's ratio is valid for small strains, i.e. linear elasticity; while for large strains, i.e. nonlinear elasticity, Poisson's function is introduced. Exemplary discussion on Poisson function can be found in (Beatty and Stalnaker 1986). The range of Poisson's ratio in isotropic elastic bodies is $-1 < \nu < 0.5$, as required by the condition of stability and thermodynamics. It is worth noticing that values from outside the said range are also possible in some anisotropic cases. For $\nu \rightarrow 0.5$ materials can change their shape relatively easily under load; however, changing their volume is almost not possible. If a body has $\nu \rightarrow -1$, it is deformed volumetrically without much difficulty; but, it is practically unachievable to change its shape. Generally, the structure of a material is responsible for the value of the Poisson ratio. For some materials structure reveals its influence on deformation properties of a material on molecular or micro level (e.g. crystals), while for some it comes into play in a meso or macro scale (e.g. foams). It is important to notice that the scale does not influence the value of Poisson's ratio for the

given material, yet, it places the phenomenon exactly where it occurs. An interesting approach to describe the mechanics behind Poisson's ratio, especially in terms of it assuming negative values, is presented in (Lakes 1991; Lakes 2002–2010).

Auxetic materials – examples, properties, applications

For most materials Poisson's ratio assumes positive values, which indulges a false intuition that if a material is stretched, it must become thinner in the cross-section. However, counter examples have been reported (Lakes 1987). Materials having negative Poisson's ratio may be called: negative Poisson's ratio materials (NPR materials), auxetics or auxetic materials (Caddock and Evans 1989), anti-rubbers (Glieck 1987), dilational materials (Milton 1992) and for foams also: re-entrants (Lakes 2002–2010).

An extensive summary enlisting examples of auxetic materials is given in (Evans and Alderson 2000). Here, let me recall only some, most common or known materials: polymer or metallic foams (Lakes 1987; Friis *et al.* 1988), microporous polymers (Caddock and Evans 1989), some natural crystals like arsenic (Gunton and Saunders 1972) or cadmium (Li 1976), natural biomaterials e.g. cat skin (Veronda and Westmann 1970), composites like carbon-fibre-reinforced epoxy composite laminate panels (Donoghue and Evans 1991).

* Department of the Strength and Fatigue of Materials and Structures, Faculty of Mechanical Engineering and Robotics, AGH University of Science and Technology, Krakow, Poland; strek@agh.edu.pl

Negative Poisson's ratio is a characteristic regarded counterintuitive, therefore very interesting especially in terms of potential applications. Materials owing such property may be used in areas where traditional solutions reveal shortcomings, exactly because of the fact that negative Poisson's ratio is followed by uncommon features. Such properties are among others: negative curvature assumed in bending – synclastic or double curvature, high resilience to indentation (both: Lakes 1987), good sound and vibration absorption (Chen and Lakes 1989, 1993, 1996; Howell *et al.* 1991), attenuation of ultrasonic signals (Alderson, Webber, Mohammed, Murphy and Evans 1997). The list of applications is in constant growth, examples are: sound insulation, air filtration, packaging, shock absorption, smart filtration, mattresses, press-fit fasteners, dilators for opening the cavity of arteries or other vessels, surgical implants, suture anchors or muscle/ligament anchors, body parts for cars and aircrafts, fiber reinforced composites, sport gear, sensor and actuator applications. The above areas of utilization are cited in (Evans and Alderson 2000), where also the detailed references to particular applications are to be found.

2. PRODUCTION OF AUXETIC FOAM

Background for the experiment

Nowadays production of auxetic materials is much more industrialised than in the beginning. First auxetic materials were produced by Lakes (Lakes 1987). He obtained auxetic polymer and metallic foams. His success consisted in the simplicity of the main idea: in order to obtain reverse properties he reversed the internal structure of the original materials; initially convex cells were converted into concave ones with symmetrically collapsed ribs.

The experiment which is described in this article followed the idea of R.S. Lakes. Generally, more than one kind of a foamed material can be changed into an auxetic in laboratory conditions, though, different foams require different manufacture techniques. For the experiment presented here, there was open cell polymer foam chosen to be processed. Specimens of the conventional open cell polymer foam were compressed in three orthogonal directions by having been placed in moulds of dimensions smaller than the initial sample size. Next, moulds with samples were heated to the temperature a little higher than the softening point of the foam; then the set-up was cooled to room temperature and the foam was taken out. The processed material exhibited auxetic behaviour, which was then examined under a microscope and in a tensile test. The results were discussed.

Naturally, many factors influence the process of production itself, as well as consequent properties of foams with negative Poisson's ratio. Among such important characteristics there should be counted: the starting material com-

position, its relative density (the density of the cellular material divided by that of the solid skeleton), temperature and time of processing, permanent volumetric compression ratio or cell size (Choi and Lakes 1992; Wang *et al.* 2001; Brandel and Lakes 2001). All the factors function together, so in order to produce foam with particular desired properties one must optimise all the design variables – for the material, as well as for the processing procedure.

Material

The material chosen for the experiment was provided by the firm "Carpenter"⁰¹. It was open-cell polyether foam with the cell size: 0.6 mm and the volumetric density: 30 kg/m³. The foam profile chart enclosed by the producer is given below in the Table 1.

Table 1

Foam profile chart with material characteristics

Quality	RP30048 Richfoam Polyether®	Standard
Colour	White / light blue	
Apparent (bulk) density brutto	30.0 kg/m ³ +/-1	EN ISO 845
Apparent (bulk) density netto	28.0 kg/m ³ +/-1	EN ISO 845
Stress-strain characteristic in compression	4.8 kPa +/-10%	EN ISO 3386
Hardness by indentation technique	180 N +/-10%	EN ISO 2439
Tensile strength	100 kPa	EN ISO 1798
Elongation at break	130%	EN ISO 1798
Compression set	<4%	EN ISO 1856
Air permeability	>10 l/min	"Carpenter" procedure
Cells per 1cm	17 +1/-2	
Fire code		MVSS 302

Moulds were cut from a copper pipe; they were 15 cm long and had the inner diameter of 3.22 cm and outer diameter of 3.5 cm. In order to hold the foam inside the pipe mould both ends of the form were blocked with iron plates of dimensions 5 cm x 5 cm. The plates were 2 mm thick; in each pair one of the plates there were 2 holes of 2 mm diameter in order to allow air escape during thermal processing. The assembly was held together by means of two ca. 17 cm long screws welded to one of the plates and put on the other.

Naturally, the relation between a mould size and a sample size is crucial, since the auxetic effect is obtained thanks to compression of the foam in the forms. Initial sample size is then determined by the dimensions of the mould and vice versa. The relation is expressed by a volumetric compression ratio (VCR). However, one should remember that the sample, after removal from the mould, may undergo a so called spring back effect and regain some of its initial volume. To count the effect in, in the presented experiment there were used the following magnitudes, as defined in (Brandel and Lakes 2001):

- the initial volumetric compression ratio – a ratio of the initial sample volume V_i over the mould volume (or: the desired final volume) V_m : $VCR_i = V_i / V_m$,
- the final volumetric compression ratio – a ratio of the initial sample volume V_i over the true final volume (after the spring back) V_f : $VCR_f = V_i / V_f$,
- the spring back effect – the difference in the desired final volume of the sample, usually the mould volume V_m , and its true final volume V_f : $SB = V_f - V_m$.

Studies showed (Choi and Lakes 1992) that for open cell polymer foams the volumetric compression ratio should be 3.3–3.7 in order to obtain minimal values of Poisson’s ratio. Nevertheless, the range of VCR suitable for successful transformation is from 2 to 5 (Lakes and Witt 2002; Wang *et al.* 2001).

Samples

The supplier submitted the material in the form of five pieces of the circular cross-section of the diameter 5 cm and the length 1 m.

The pieces were cut using a cutter and scissors to samples of the dimensions about: length – 21.8 cm, diameter – 5 cm (without change). These dimensions were chosen with regard to the mould dimensions in order to obtain the initial compression ratio of the optimal value $VCR_i = 3.46$ (on average). There were 12 samples studied plus two trial samples: No. 01 and 02. The trial sample No. 1 was used for calibration of heating temperature and the thermal process duration, while the No. 02 was unprocessed and was used for comparison.

By inserting a sample into a mould one has to remember about uniform distribution of stress and avoiding wrinkles.

In the presented experiment 6 foam specimens were put into moulds with the use of petroleum jelly (“MelkFett”) as a lubricant in order to help in easier squeezing into the forms. Other 6 specimens were put in the moulds without the lubricant. Before heating, samples in moulds were allowed “resting” for couple of minutes so that compression stress was distributed uniformly.

Thermal process

The processing temperature has to be equal or slightly greater than the material’s softening point and remains in a strict relation to the processing time. Too low the temperature or not sufficient duration of the treatment can result in an incomplete transition of specimens. On the other hand, excessive heat or time can cause cell ribs to adhere to each other. However, some alternations like higher temperature combined with shorter time are also possible.

There are two ways of proceeding after accomplishing the thermal treatment. One is to extract the specimen of the mould immediately after taking it out from the furnace (Brandel and Lakes 2001) and the other is to allow the mould with the sample inside to cool at room temperature and only then extract the specimen (Wang *et al.* 2001). The removed sample should be stretched a little bit to separate possibly adhering ribs. It is also advisable to wait some time before proceeding with measurements to allow the potential recovery effect to occur.

Neither did the firm “Carpenter” supply data regarding melting temperature, nor was differential scanning calorimetry performed. Softening point was to be found experimentally and temperatures ranging 104–190 °C, as well as different processing time values from 10 to 50 minutes, were exercised. At the beginning, the trial sample (No. 01) was multiply heated at various temperatures in order to find optimal processing conditions. These turned out to be 30–50 min and 170–190 °C, which is most probably due to rather thick moulds and large sample dimensions. The thermal process was conducted in a laboratory furnace. After completion of the heating procedure samples were taken out and left in forms till complete cooling.

The Table 2 below shows details of the thermal process.

Table 2
 Processing conditions of samples

Sample No.	01				02	not processed											
	t [min]	10	20	25		30	1 / 28 VI 2005	2 / 28 VI 2005	3 / 28 VI 2005	4 / 28 VI 2005	5 / 28 VI 2005	6 / 28 VI 2005	7 / 28 VI 2005	8 / 28 VI 2005	1 / 1 VII 2005	2 / 1 VII 2005	3 / 1 VII 2005
Time	t [min]	10	20	25	30	30	30	50	50	30	30	40	40	45	45	45	45
Temp.	T [°C]	104	120	150	170	170	170	170	170	190	190	190	190	190	190	190	190

Results

When samples regained room temperature they were taken out and, in order to obtain stable results all specimens were left for three days before further study.

Despite careful preparation of samples, less than half of all processed foam pieces possessed wrinkles or other transformation imperfections like bends. It turned out that the petroleum jelly had almost no influence on the squeezing and therefore on the presence of wrinkles. Most of the samples exhibited the auxetic effect, but some of the foam pieces underwent complete transition while some were auxetic only in part. This is attributed to the fact that samples were processed under different time and temperature conditions, as well as to uneven squeezing or stress distribution.

At this stage of the experiment auxetic effect was observed by the assessment of volumetric compression ratios. Sample dimensions were measured with a micrometer at the following stages: before the thermal processing, just after quenching and 3 days after thermal procedures. All measurements were done 3 times and mean values were later used for calculations. The best auxetic effect was obtained for samples showing least differences between initial and final VCRs, that is for samples processed for 45 minutes in 190 °C. The Figure 1 below shows how samples underwent the spring back effect.

Symbols used in the graph expand as follows:

- $VCR_i = V_i / V_m$ – the initial VCR; the initial sample volume V_i over the mould volume V_m ,
- $VCR_{f0} = V_i / V_{f0}$ – VCR just after quenching; the initial sample volume V_i over the volume after quenching V_{f0} ,
- $VCR_f = V_i / V_f$ – the final VCR; the initial sample volume V_i over the final volume V_f .

3. MICROSCOPIC OBSERVATIONS

Preparation of samples for microscopic observations

The produced foam underwent another qualitative assessment in terms of achieving the auxetic effect by observation of the material structure in a micro scale. Microscopic imagery was also used to study structural mechanisms, i.e. to show how cell ribs behaved when a sample was compressed and pulled. It was expected that the processed material would show to have concave cells that would unfold under tension, therefore producing growth of the specimen volume, while in compression the internal structure would collapse inwards and increase density in this way. For comparison, the unprocessed foam was expected to show normal convex cells that would elongate and thin with tension and buckle in compression.

Before proceeding with microscopic imagery, samples needed to be properly prepared; this included cutting to the desired shape and dimensions. In general, a cutting method depends on the stiffness of the re-entrant and desired sample dimensions. In the case of the presented experiment specimens were cut using a steel cutter.

Two samples (NPR and unprocessed) were prepared; specimens were about 1 cm thick, 5 cm long and of width about 4 and 3 cm for regular and auxetic material respectively. The re-entrant specimen was cut out from the sample 8/28 VI 2005 (the final volumetric compression ratio: $VCR_f = 3.22$). Both specimens were placed in a specially built form where they were stretched and compressed. Stretching was performed at 8%, 15% and 30% strain. Compression was performed only to show general changes in structure without precise reference to strain value; since it was impossible to evaluate strain because of buckling of the relatively long samples. Images were taken with the Olympus DP10 Digital Camera from the Olympus BH2 Light Microscope with 12.5 magnifying factor.

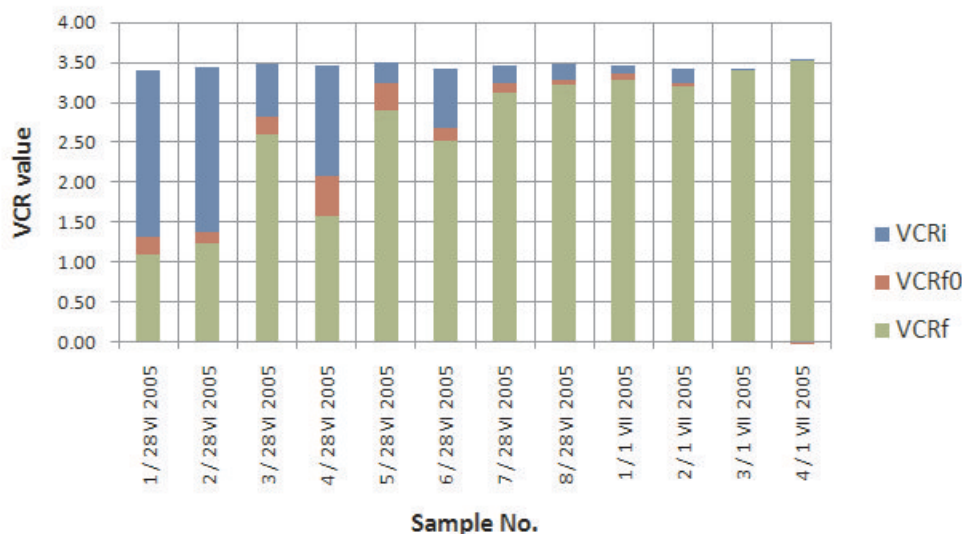


Fig. 1. Volumetric compression ratios. Samples processed longer in higher temperatures show smaller spring back effect

Results – geometrical characteristics

Intrinsic features of traditional and auxetic materials were evaluated with the use of photos in 0% strain (Figs. 2–5). As for the unprocessed foam, the cell shape was convex, but irregular, with faces of penta- and hexagons, occasionally other geometric figures. Cell diameter was difficult to be measured directly, since faces of cells differed in size (from small tetragons of 250 μm in diagonal to large octagons of 700 μm in diagonal). Mean diagonal value for faces was then about 475 μm . The diameter of cells, due to the data provided by the manufacturer was 600 μm . Cell ribs were straight, connected in vertices. Connectivity, that is the number of cell edges that meet at a node or vertex, was mostly 3, in some vertices 5. Thickness of ribs was 50–60 μm and length: 160–270 μm . As far as the uniformity of geometry is concerned, since cells are formed from heterogeneous shapes, the anisotropy on the level of microscopic exactness can be seen, however, regarded macroscopically, the material is isotropic.

Similarly, characteristics of the re-entrant foam were also determined as follows. Cell shape was found concave, irregular, cells folded and congested, no apparent shapes could be distinguished. Cell diameter was impossible to be evaluated directly, diagonals of faces varied from 160 to 520 μm . Mean diagonal value for faces was then about 340 μm . The diameter of cells evaluated from the data provided by the manufacturer for the regular foam and the linear compression ratio was 445 μm . Cell ribs folded in different directions, connected in vertices (connectivity: 3 to 5). Thickness of ribs was 50–60 μm , their length was im-

possible to be stated exactly, average value was about 210 μm . Cells were irregular, which implied anisotropy on the level of microscopic exactness; however, regarded macroscopically, the material was isotropic.

Results – deformation mechanisms

Mechanisms of deformation under applied stress can be seen in sequential photos below (Figs. 2–5). All microscope photos are to the same scale (12-fold magnification), which is indicated with the mark bar (1000 μm) in the photos. The broken ribs which can be seen in the photos are located on the edges of specimens, they did not break as consequence of strain but were cut during cutting out samples.

The first sequence (Fig. 2) shows how internal structure of the regular foam responds to tensile strain. Cells elongate and become thinner in the axis perpendicular to the axis of deformation. The next sequence (Fig. 3) presents how auxetic foam responds to strain: cells unfold and grow bigger under tension. It is assumed that prevailing mechanisms are rib bending and then rib elongation in the direction of stretching. The third sequence (Fig. 4) reveals that the mechanism of deformation of the regular foam under compression consists in rib bending and rib buckling. The strain in the left picture was above the linear elastic region (about 30%). And finally, the fourth sequence (Fig. 5) proves that mechanisms governing deformation in auxetics are difficult to be observed. It is assumed that cell ribs undergo bending and inward folding. Certain degree of densification can also be seen as the ribs come closer to each other under compression.

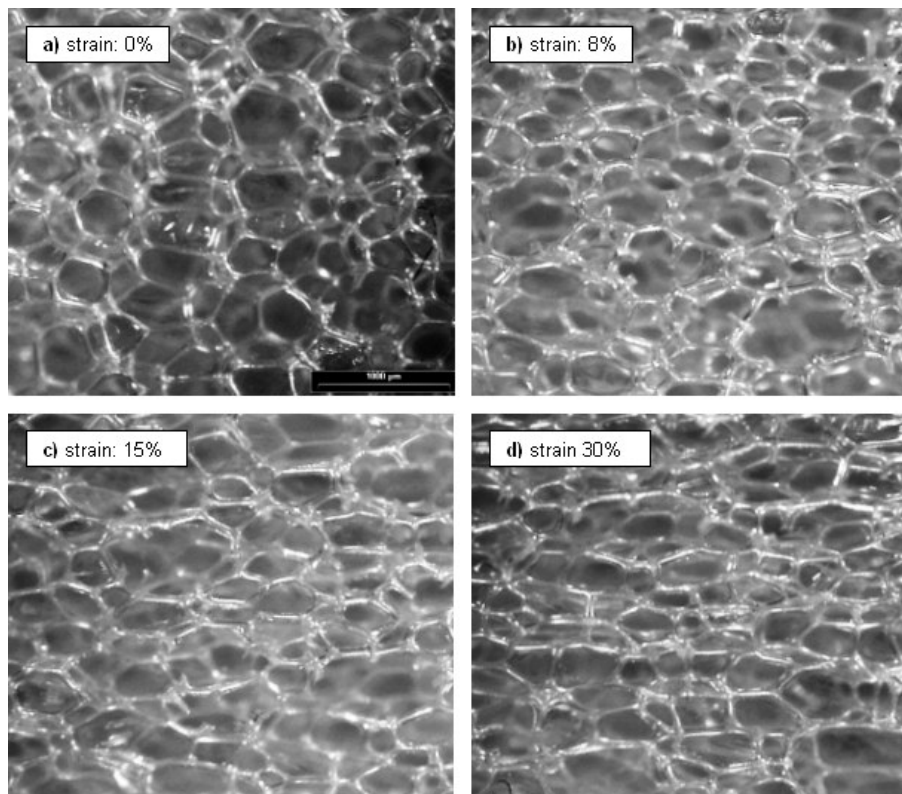


Fig. 2. Regular (unprocessed) foam under tension

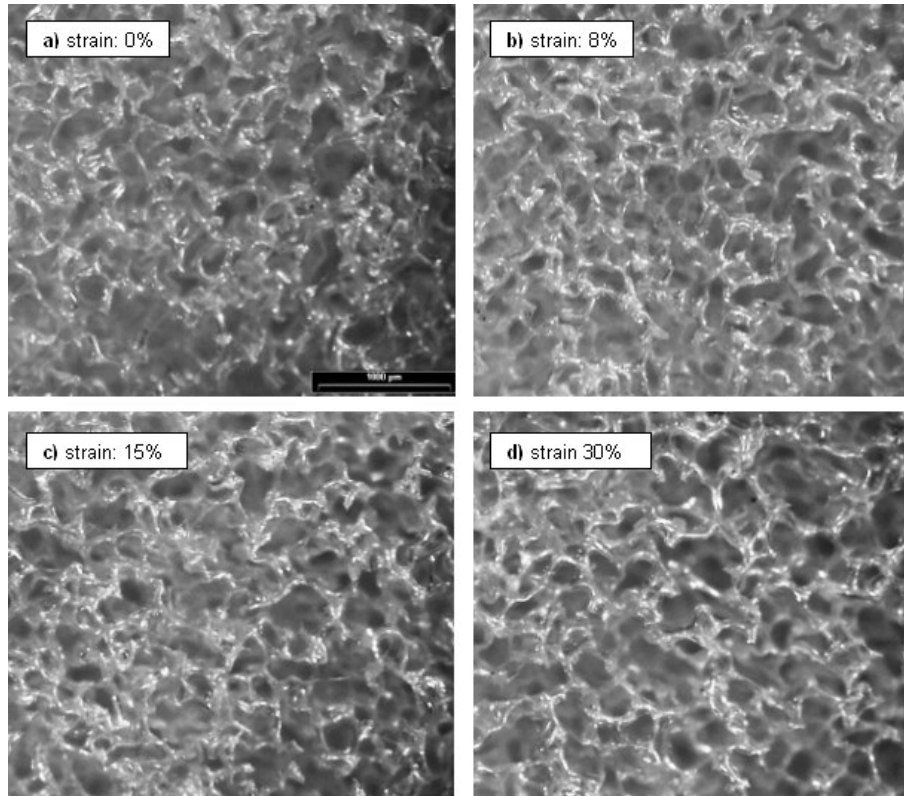


Fig. 3. Auxetic foam under tension

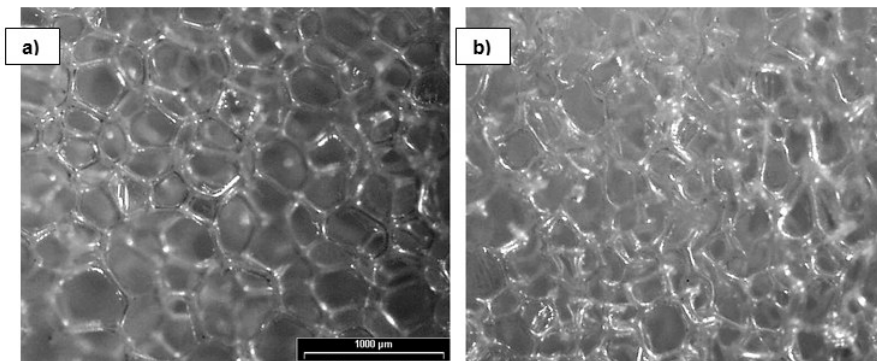


Fig. 4. Regular (unprocessed) foam under compression: a) no strain; b) compressed

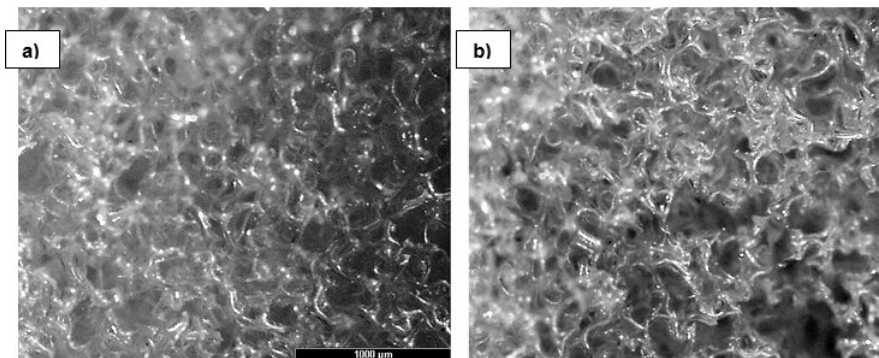


Fig. 5. Auxetic foam under compression: a) no strain; b) compressed

4. MECHANICAL PROPERTIES

Preparation of samples and testing procedure

After qualitative assessment of the auxetic effect in the produced foams, a more detailed study was performed in order to find numerical values of the Poisson ratio. The tests consisted in loading samples with longitudinal tension and measuring of stress and longitudinal and lateral strains. Longitudinal stress and strain were measured by the tensile machine, while lateral deformation was determined in an optical method, by analysis of sequential photos of samples under specified load. The data from tests were processed in order to obtain: Poisson's ratio, stress-strain curves (using engineering values), stress-strain curves (using true values).

It was decided to test specimens with visibly varying behavior. Four samples were taken: two exhibiting distinct negative Poisson's ratio and two showing no or little auxetic effect. Also a sample of the not processed material was tested for comparison. Due to the fact that the specimens had visibly different properties and their small number (5 in total) statistical numerical analysis was omitted and the uncertainty was assumed based on practical premises (see below in: *Results – Poisson's ratio*).

From each of the five samples smaller specimens of dimensions 50 × 10 × 10 mm were cut out using a steel cutter. Each specimen had a mesh of reference points applied on one of the four faces; the mesh was to be used for determination of lateral deformation. The meshes were applied in the middle area of the samples so that their deformation was not affected by uneven stress distribution or fixing to the machine.

Samples were glued to the machine holds with the UHU® glue. As it proved during testing, most samples failed in place of the glued connections; this was attributed to the fact that the glue could have destroyed some of foam ribs. However, samples held long enough to perform the desired observations. The machine used was TIRAtest

28100 with the software available for it. All results were then converted into the Excel® format data.

It was decided to put samples under the following testing conditions: displacement rate: 0.2 mm/s with a pause for 10 seconds after every 4% (=2 mm) longitudinal deformation until 40% and a pause for 10 seconds after every 15% (=7.5 mm) longitudinal deformation from 40% until failure or 190%. The total range of deformation was from 0% to failure or 205%.

During each loading pause photos were taken using the camera Sony® Cyber-shot™ 5.0 Mpix DSC-V1 (sensor size 7.18 × 5.32 mm). The photos were saved as JPEG files in the resolution 2592 × 1944 (True Color RGB mode) and processed later using Adobe Photoshop® 7.0.

During testing one of the samples the pause at 160% and 175% strain was extended to 5 minutes in order to observe the potential for relaxation of the foam.

Results – Poisson's ratio

As stated before, during tensile tests photos were taken at certain values of longitudinal strain. Displacement of mesh points was the basis for calculation of deformation and later Poisson's ratios at sequential strains. The processing of photos consisted in finding and marking the reference points in sequential pictures and denoting their coordinates in pixels. Calculation of Poisson's ratios was performed with the use of Mathcad® 2001. The procedure returned Poisson's ratios with error regions, that is with their maximum and minimum possible values, according to the assumed uncertainty. The uncertainty was assumed due to the following factors: perspective and distortion effects, random micro-movements of the photo camera during pressing the shutter button and random omissions in case of reading from the blurred regions.

Below is given a plot showing Poisson's ratios versus engineering strains for all tested samples (Fig. 6). For the clarity of the graph error regions are not shown.

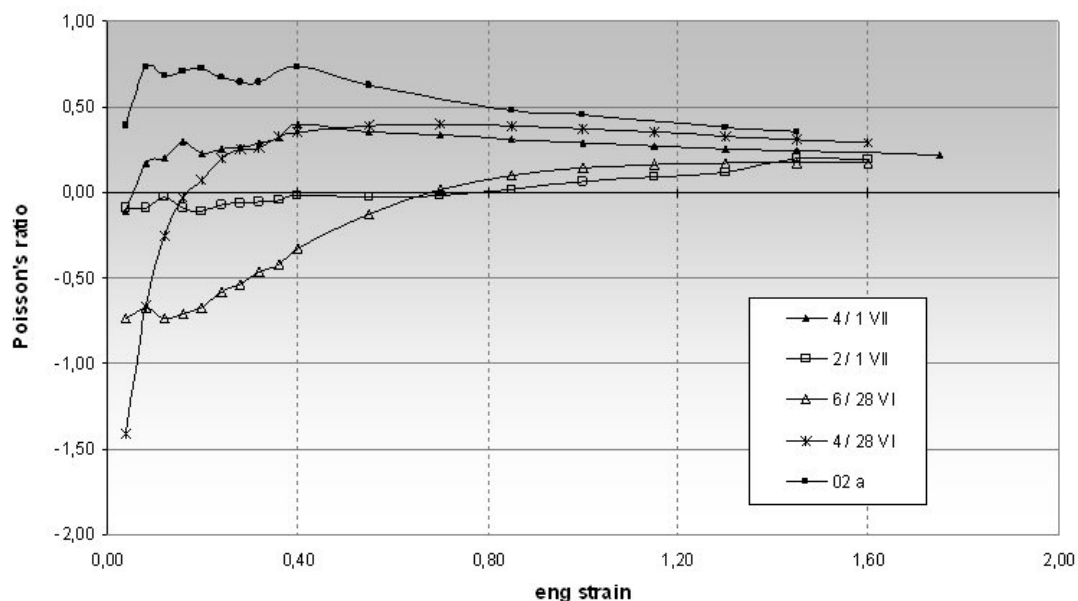


Fig. 6. Poisson's ratio depending on engineering strain

An overall conclusion at this stage is that best processing conditions in order to obtain the strongest auxetic effect for the studied foam were: temperature about 190 °C, time about 30 to 40 min. Also, it is worth of notice that generally polymer foams are viscoelastic materials, i.e. their Poisson's ratio may vary with time. Some experiments at small strains disclosed that viscoelastic effects are sufficiently small not to affect the studies of dependency of Poisson's ratio on strain (Choi and Lakes 1992).

Results – engineering and true stress-strain relations

Measurements in the tensile tests were done for all elongations by steps equal to 0.01% longitudinal deformation. The data included engineering values of longitudinal strain and respective stress; that is values disregarding change of the cross-section area due to elongation. True stress and strain values can be obtained from the formulae from (Choi

and Lakes 1992): $\sigma_{\text{true}} = \sigma / (1 - \nu \epsilon)^2$ and $\epsilon_{\text{true}} = \ln(1 + \epsilon)$, in which σ_{true} is true stress, ϵ_{true} – true strain, σ – engineering stress, ϵ – engineering longitudinal strain, ν – Poisson's ratio.

There were analyzed graphs depicting engineering stress-strain relations derived from the unprocessed data. The graphs showed characteristic drops of stress (compare: Figs. 7a and 7b – an exemplary plot of the unprocessed data). This effect occurred due to the pauses in pulling of samples made for taking the photos. As can be inferred from these considerable decreases in stress, relaxation might have occurred. On the other hand, it might be also that some of cell ribs broke causing the drops. Two of the pauses (at 160% and 175% elongation) for the sample 2/1 VII 2005 were lengthened to 5 min and as can be seen the decreases in stress are significant. Nevertheless, viscoelastic effects were not yet the subject of the study and so they are only denoted here without further investigation.

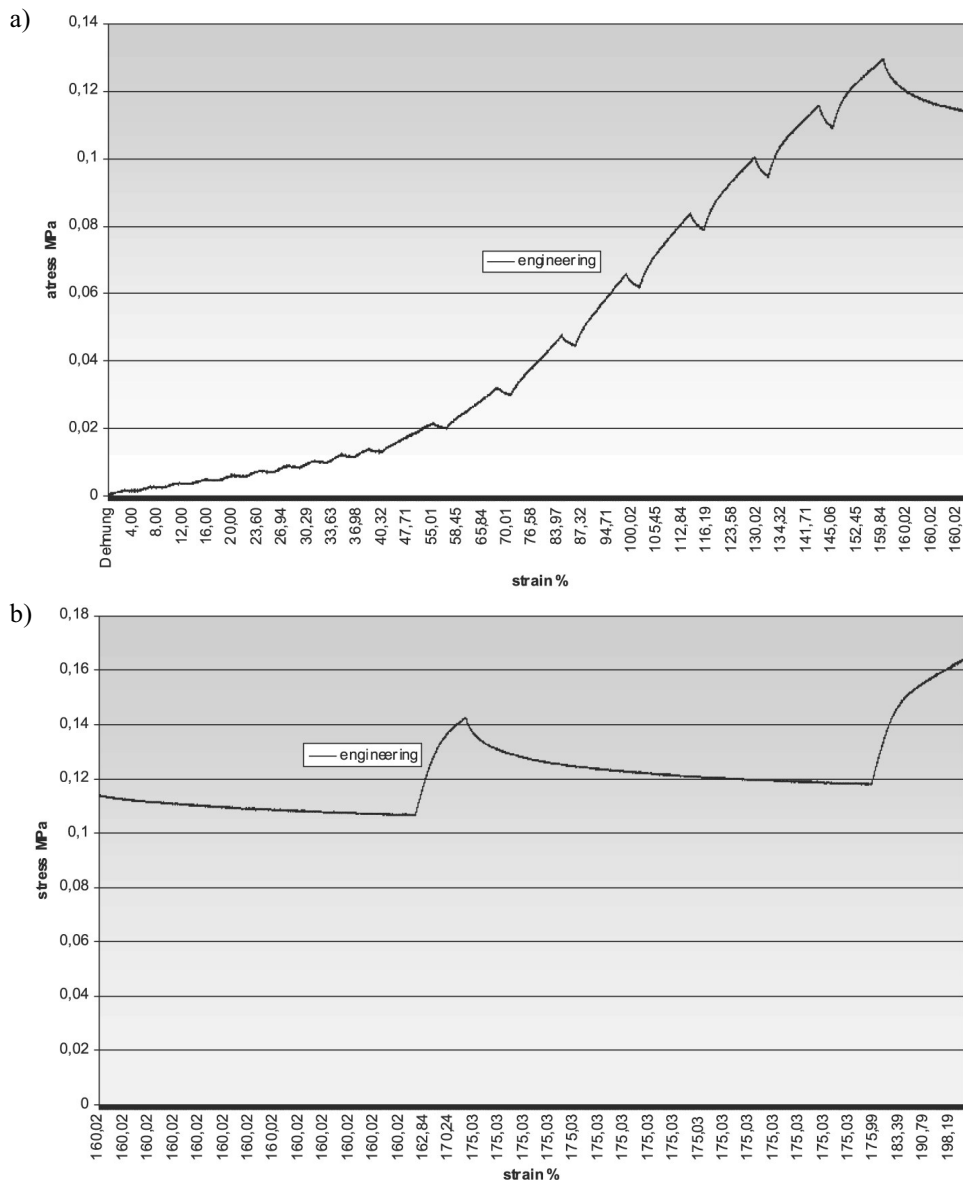


Fig. 7. Stress-strain diagram for the sample 2/1 VII 2005: a) part one; characteristic drops of stress due to the pauses in pulling of the sample made for taking the photos; b) part two; characteristic drops of stress due to the pauses in pulling of the sample made for taking the photos

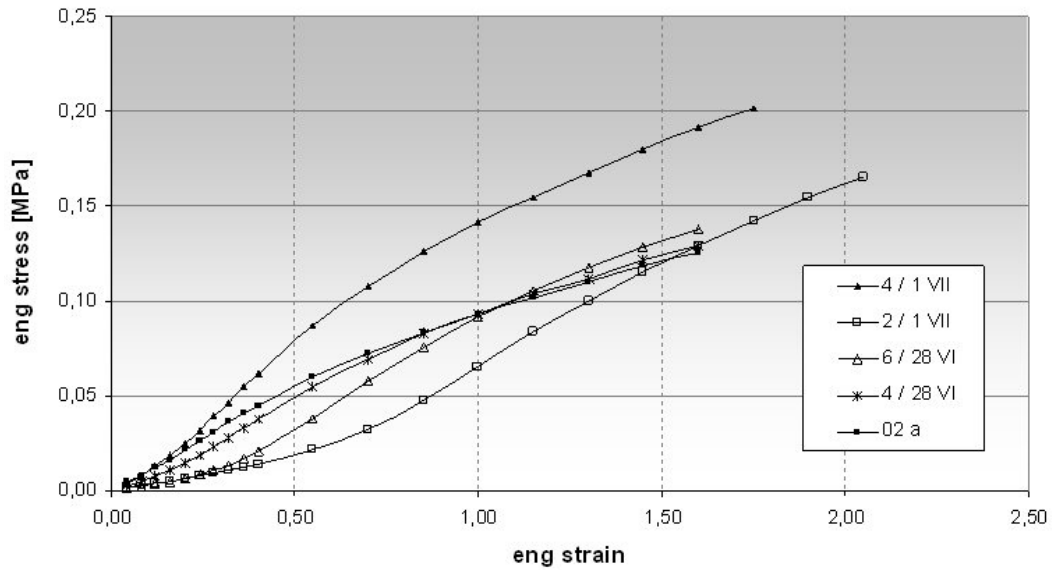


Fig. 8. Engineering stress-strain dependency

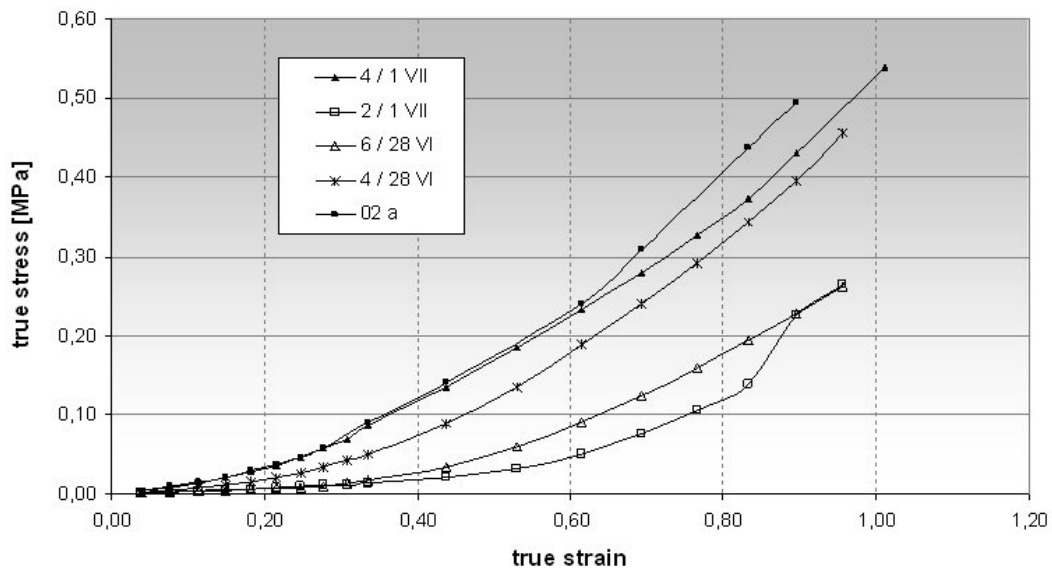


Fig. 9. Trend lines for true stress-strain relations

In order to obtain somewhat more illustrative graphs the data from the tensile tests were processed. The method to obtain smooth curves was to isolate the data for exact elongations: at 4%, 8% and so on until 40% by the step of 4% and later from 40% until 160(175)% every 15%. The isolated points were then linked by a smooth curve giving in this way a trend line for engineering stress-strain dependency, based on actual discrete results (Fig. 8). True stress-strain relations were obtained by converting the discrete numerical values by the formulae cited above, results are plotted in the Figure 9.

5. FINAL REMARKS

Materials with negative Poisson's ratio are still regarded as counterintuitive and in spite of their interesting properties

not well known. Auxetic foams can be produced in laboratory conditions; polymer foams need thermal processing of compressed samples in order to transform into re-entrant material.

The experiment proved that best NPR effects for the used foam were temperature about 190 °C and time about 30 to 40 min. Appropriate microscopic observations and mechanical tests provided data for determination of internal structure and deformation manner. The data obtained from tensile tests and photos made during stretching were basis for calculation of Poisson's ratio. The tensile tests provided results for both engineering and true stress-strain relations. Additionally, tested materials showed considerable capacity for relaxation. Viscoelastic effects should be investigated in detail in the future.

Acknowledgments

I would like to kindly thank professor Ryszard B. Peçherski for his contribution to the final shape of the article.

The article was written based on the experiment done and material gathered for the master thesis "Mechanical properties of materials with negative Poisson's ratio. Based on own experimental investigations of auxetic polymer foam". The thesis was prepared at the Chair of Strength of Materials, the Institute of Structural Mechanics in the Department of Civil Engineering, the Cracow University of Technology under the supervision of professor Ryszard B. Peçherski and with the cooperation of Prof. Dr.-Ing. habil. Tom Schanz and Dr. Maria Datcheva, from the Institute of Soil Mechanics, the Department of Civil Engineering at the Bauhaus-Universität Weimar, within the framework of the Socrates-ERASMUS programme.

References

- Alderson K.L., Webber R.S., Mohammed U.F., Murphy E., Evans K.E. 1997, *An Experimental Study of Ultrasonic Attenuation in Microporous Polyethylene*. Applied Acoustics, vol. 50, No. 1, January 1997, pp. 23–33(11).
- Baur, W.H. 2003, *Microporous materials: frameworks under pressure*. Nature Materials, vol. 2, Issue 1, pp. 17–18.
- Beatty M.F., Stalnaker D.O. 1986, *The Poisson Function of Finite Elasticity*. Journal of Applied Mechanics, vol. 53, Issue 4, December 1986, pp. 807–813.
- Brandel B., Lakes R.S. 2001, *Negative Poisson's ratio polyethylene foams*. Journal of Materials Science, vol. 36, No. 24, July 2001, pp. 3885–5893.
- Caddock B.D., Evans K.E. 1989, *Microporous materials with negative Poisson's ratio: I. Microstructure and mechanical properties*. Journal of Physics D: Applied Physics, vol. 22, No. 12, pp. 1877–1882.
- Chen C.P., Lakes R.S. 1989, *Dynamic wave dispersion and loss properties of conventional and negative Poisson's ratio polymeric cellular materials*. Cellular Polymers, No. 8(5), pp. 343–59.
- Chen C.P., Lakes R.S. 1993, *Viscoelastic behavior of composite materials with conventional- or negative-Poisson's-ratio foam as one phase*. Journal of Materials Science, vol. 28, No. 16, pp. 4288–98.
- Chen C.P., Lakes R.S. 1996, *Micromechanical analysis of dynamic behavior of conventional and negative Poisson's ratio foams*. Journal of Engineering Materials and Technology, vol. 118, Issue 3, pp. 285–288.
- Choi J.B., Lakes R.S. 1992, *Nonlinear properties of polymer cellular materials with a negative Poisson's ratio*. Journal of Material Science, vol. 27, No. 17, pp. 4679–4684.
- Donoghue J.P., Evans K.E. 1991, *Composite laminates with enhanced indentation and fracture resistance due to negative Poisson's ratio*. W.S. Tsai, & G. Springer, Proceedings of 8th International Conference on Composite Materials (ICCM-8), pages 2-K-1–2-K-10. Honolulu, Hawaii: Society for the Advancement of Material and Process Engineering (SAMPE), Covina, CA.
- Evans K.E., Alderson A. 2000, *Auxetic Materials: Functional Materials and Structures from Lateral Thinking!* Advanced Materials, vol. 12, Issue 9, pp. 617–628.
- Friis E.A., Lakes R.S., Park J.B. 1988, *Negative Poisson's ratio polymeric and metallic foams*. Journal of Materials Science, vol. 23, pp. 4406–4414.
- Glieck J. 1987, April 14, The New York Times.
- Gunton D.J., Saunders G.A. 1972, *The Young's modulus and Poisson's ratio of arsenic, antimony and bismuth*. Journal of Materials Science, vol. 7, No. 9, pp. 1061–1068.
- Howell B., Prendergast P., Hansen L. 1991, *Acoustic Behavior of Negative Poisson's Ratio Materials*. Annapolis, MD: David Taylor Research Centre.
- Lakes R.S. 1991, *Deformation mechanisms in negative Poisson's ratio materials: structural aspects*. Journal of Material Science, vol. 26, No. 9, pp. 2287–2292.
- Lakes R.S. 1987, *Foam structures with a negative Poisson's ratio*. Science vol. 235, No. 4792, pp. 1038–1040.
- Lakes R.S. 2002–2010, <http://silver.neep.wisc.edu/~lakes/>. Date of last opening 17th March 2010.
- Lakes R.S. 2002–2010, *What is Poisson's ratio?* <http://silver.neep.wisc.edu/~lakes/PoissonIntro.html>. Date of last opening 4th March 2010.
- Lakes R.S., Witt R. 2002, *Making and characterizing negative Poisson's ratio materials*. International Journal of Mechanical Engineering Education, vol. 30, No. 1, pp. 50–58.
- Li Y. 1976, *The anisotropic behavior of Poisson's ratio, Young's modulus, and shear modulus in hexagonal materials*. Physica Status Solidi (a), vol. 38, Issue 1, pp. 171–175.
- Milton G. 1992, *Composite materials with Poisson's ratios close to -1*. Journal of the Mechanics and Physics of Solids, vol. 40, Issue 5, pp. 1105–1137.
- Veronda D.R., Westmann R.A. 1970, *Mechanical characterization of skin-finite deformation*. Journal of Biomechanics 3, vol. 19, pp. 111–124.
- Wang Y.-C., Lakes R.S., Butenhoff A. 2001, *Influence of Cell Size on Re-Entrant Transformation of Negative Poisson's Ratio Reticulated Polyurethane Foams*. Cellular Polymers, vol. 20, Issue 6, pp. 373–385.